

<https://doi.org/10.1038/s41545-025-00500-3>

Methylmercury carbon isotope fractionation during biotic methylation by the bacterial BerOc1 strain



Luisa M. Malberti-Quintero¹ ✉, Jin-Ping Xue², Remy Guyoneaud², Alina Kleindienst², Christelle Lagane¹, Laure Laffont¹, Jeroen E. Sonke¹, Zoyne Pedrero², Emmanuel Tessier², David Amouroux² & David Point¹ ✉

Biotic methylation of inorganic mercury (iHg) in aquatic systems is largely driven by microorganisms such as sulfate-reducing bacteria (SRB). Using the SRB model strain *Pseudodesulfovibrio hydrargyri* BerOc1 we investigated biotic iHg methylation aiming to assess the rates of mono-methylmercury (CH₃Hg) production and to characterize the carbon (C) isotopic signatures ($\delta^{13}\text{C}$) of the CH₃Hg product. Biogenic CH₃Hg exhibited $\delta^{13}\text{C}$ values averaging $-23.1 \pm 2.0\text{‰}$, representing a ¹³C-depletion of 14.4‰ compared to the pyruvate carbon source used for the growing of the strain and a 9‰ depletion relative to the microbial biomass. The maximum methylation yield observed in our samples was around 15% of the available iHg and a constant C isotope fractionation was detected over time. We propose that the methyl group is metabolically transferred from the carbon sources to cobalamin in the HgcA protein and subsequently to inorganic mercury (iHg), leading to consistent light C isotope enriched CH₃Hg signatures.

Sulfate-Reducing Bacteria (SRB) are among the most extensively studied organisms capable of methylating inorganic mercury (iHg)^{1,2}. Over the past few decades, SRBs have been recognized for their significant contribution to microbial Hg methylation, with at least 36 Hg-methylating strains identified to date³. These bacteria thrive in anoxic environments, such as sediments and wetlands, where they perform anaerobic respiration by using sulfate (SO₄²⁻) as the terminal electron acceptor in their electron transport chain, rather than oxygen^{4,5}. Some sulfate-reducing microorganisms can also use alternative electron acceptors, such as fumarate, nitrate, nitrite, ferric iron, and dimethyl sulfoxide, and can use acetic acid, lactic acid, and pyruvate as electron donors^{6,7}. Importantly, the sulfate reduction process is dissimilatory⁸, meaning it is not used for cellular biosynthesis, but rather to generate metabolic energy (electrons) for the cells.

In anoxic environments, SRBs play a key role in the degradation of organic matter and, in the process, can convert iHg into mono-methylmercury (CH₃Hg)^{9–11}. This transformation involves the interaction of iHg with bacterial enzymes, facilitating the transfer of a methyl group from a donor, currently identified as the corrinoid protein HgcA^{12,13}, to iHg^{14,15}. Mono-methylmercury (CH₃Hg) production by SRBs is typically enhanced in environments rich in organic matter, which supports microbial activity¹⁶. However, the extent of methylation (% of bioavailable iHg converted to

CH₃Hg) varies based on environmental conditions, including pH, temperature, and organic carbon availability¹⁷.

Studies have shown that the methylation capacity of SRBs is strain-dependent^{18–20} and is influenced by growth conditions, such as sulfate reduction or fumarate respiration²¹. Strains from the (*Pseudo*)*Desulfovibrio* genus are frequently used as model organisms to investigate the mechanisms of mercury methylation, in particular the *Pseudodesulfovibrio hydrargyri* BerOc1 strain^{11,20–23}. This strain has recently been proposed as type *Pseudodesulfovibrio hydrargyri* sp. nov²². Previously, it was classified as *Desulfovibrio caledoniensis*¹⁸ and *Desulfovibrio dechloroacetivorans*²¹, and these names can still be found in earlier literature.

The BerOc1 strain, first identified as capable of methylating iHg in 2009¹⁸, has since become a key model strain for studying biotic methylation of Hg. Its genome has been publicly available in databases under access number LKAQ00000000²⁴. BerOc1 has been extensively studied to explore various aspects of Hg biomethylation, including the mechanisms of intracellular Hg transport and methylation sites²⁵, the relationships with energetic metabolism²¹ or Hg isotopic fractionation during biomethylation²⁶.

BerOc1 cells are small, motile, curved-rod vibrios, and are strictly anaerobic. The strain grows through sulfate reduction, fumarate respiration, and pyruvate fermentation, utilizing lactate, pyruvate, and ethanol as carbon sources, but it seems not to use many other common substrates²². BerOc1

¹Géosciences Environnement Toulouse, CNRS/IRD/Université, Toulouse III- Paul Sabatier, Toulouse, France. ²Université de Pau et des Pays de l'Adour, CNRS, Institute of Analytical Sciences and Physical-Chemistry for the Environment and Materials—IPREM, Pau, France. ✉e-mail: lmalberti1996@gmail.com; david.point@ird.fr

can both methylate iHg and demethylate CH₃Hg, although the *Mer* operon, which is typically linked to CH₃Hg demethylation, has not been identified in its genome²⁴. Nonetheless, CH₃Hg demethylation has been reported in various studies^{19,22,25,26}. The strain's iHg methylation potential is significantly influenced by growth conditions, with maximum activity reported under fumarate respiration^{21,23}. Under non-sulfidogenic growth, BerOc1 has shown a methylation potential ranging from less than 2% to approximately 35% of iHg, depending on factors such as the initial iHg concentration and the presence of sulfur-containing compounds like cysteine or sulfide in the growth media²³.

Hg stable isotopes, which display both mass-dependent and mass-independent fractionation, are powerful tools for tracing Hg sources and understanding transformation pathways in natural environments^{27,28}. Research indicates that microbial methylation of inorganic Hg produces distinct Hg isotopic signatures largely unaffected by environmental conditions or the type of methylating bacteria^{26,29}. This consistency suggests a shared enzymatic mechanism, likely involving the *hgcA* and *hgcB* genes^{13,29}. To accurately interpret these processes, species-specific isotopic analyses within cellular fractions are crucial for unraveling the complexity of intracellular Hg transformations. In the case of CH₃Hg, analyzing the stable isotopes of carbon ($\delta^{13}\text{C}$) potentially offers additional insight into the origin and metabolic transformations of the methyl group. However, such studies have been limited by technical challenges, including the need for high CH₃Hg concentrations and simple matrices. Recent methodological advancements, particularly the development of purge and trap–gas chromatography–combustion–isotope ratio mass spectrometry (PT-GC-C-IRMS)^{30,31}, have helped overcome these limitations, enabling carbon (C) isotope analysis of CH₃Hg and, more recently, the characterization of C isotope fractionation during CH₃Hg photodemethylation³².

Despite the advances in understanding the genetic traits related to iHg methylation¹³, the full metabolic pathway or biological cause for the methylation is not yet fully understood and the connections between the C source, methyl group donors, and the CH₃Hg product have not been established beyond the theory^{13,33}. For the present study, *Pseudodesulfobacterium hydargyri* BerOc1 was selected to investigate the biotic methylation of iHg. The primary objectives were to assess the rates of CH₃Hg production under fumarate respiration using pyruvate as the C source, characterize the C isotopic signatures ($\delta^{13}\text{C}$) of the resulting methylated Hg products, and discuss if C isotopes are useful to understand methylation pathways in the cell.

Results

Reaction yields and kinetics

Methylation yields, reaction products, and reaction kinetics were analyzed from the CH₃Hg samples obtained from the two experiments following the considerations mentioned in the calculations section. In the first biotic methylation experiment, 15% of the THg measured was in the form of CH₃Hg after 24 h of incubation, while in the second experiment, the maximum yield observed was approximately 9% after 30 h. The difference in methylation yields between the two experiments was attributed to the higher biomass production (ΔOD_{600}) during BME#1 (~0.2) compared to BME#2 (~0.11), despite the growth rates (μ) being similar (~0.050 h⁻¹ for BME#1 and 0.046 h⁻¹ for BME#2). The correlation between methylation potential and biomass production has been documented for BerOc1^{23,26} as well as for other bacterial strains^{18,34}. An example of both methylation rate (k_m) calculation and biomass production (ΔOD_{600}) corresponding to the experiment BME#2 is shown in Fig. S1 of the Supplementary Information (S1).

The inherent variability in biomass production and differences in reaction models make direct comparisons between kinetics from different studies challenging. As a result, a descriptive approach is commonly used to compare outcomes. In BME#2, triplicate samples at each time point showed excellent reproducibility in the percentage of methylation detected, and a linear increase in CH₃Hg concentration was observed over time (see Fig. S1.A). The methylation rate constant for BME#2 was calculated using Eq. 2,

yielding a value of $k_m = 3.27 (\pm 0.03, \text{SE}) \times 10^{-3} \text{ h}^{-1}$. This k_m value is of the same order of magnitude as reported in previous studies involving strain cultures of SRB¹⁹ and using BerOc1 under high salinity conditions^{23,26}.

As a comparison, this rate also aligns closely with results from Rodríguez Martín-Doimeadios et al. (2004)³⁵ on natural biotic methylation in anoxic sediments from the Adour River estuary in France ($k_m = 2.27 (\pm 0.10, \text{SE}) \times 10^{-3} \text{ h}^{-1,35}$). In that study, surface intertidal sediment (0–5 cm) was used, and it was noted that demethylation rates were 10 times lower than methylation rates during 1-day incubations. However, it is important to recognize that natural sediments contain diverse bacterial strains, potentially contributing differently to methylation and demethylation processes.

In terms of methylated products, only CH₃Hg was detected in all samples, with no evidence of dimethyl Hg ((CH₃)₂Hg) formation. This is consistent with previous studies using BerOc1, where CH₃Hg has been the sole observed methylated species²⁶.

Although numerous studies have demonstrated that iHg methylation is an intracellular process^{13,20,34} and that the assimilation of iHg by microorganisms is a critical step in this process³⁴, it is essential to confirm that the CH₃Hg produced in our experiments is entirely of biological origin and not the result of abiotic methylation with organic components present in the culture medium or even the cell walls. The biotic origin of the CH₃Hg observed in our samples was confirmed through two types of control experiments. The first control involved triplicate samples with active cells and iHg addition, which were acidified at $t = 0$. These samples contained all the organic compounds and non-enzymatic methylating agents present in the solution, providing a good indication of whether abiotic methylation was occurring. The second control consisted of triplicate samples with inactive cells and iHg addition, incubated under the same conditions as the experimental samples. After 30 h of incubation, these samples were acidified, and mercury speciation was measured. In both controls, negligible CH₃Hg was detected during the Hg speciation analysis, suggesting that all CH₃Hg produced in our experiments was the result of biological activity. The iHg methylation percentages observed in all the samples studied is summarized in Table S1 of the SI material.

Carbon isotope signatures from CH₃Hg and C sources

The C stable isotopes of the biotically produced CH₃Hg were analyzed, excluding the 4 h incubation samples due to insufficient CH₃Hg concentration for CH₃Hg $\delta^{13}\text{C}$ -CSIA. Since these samples lacked a reference point and yielded low concentrations after purification, the $\delta^{13}\text{C}$ of the 15% methylated sample (the highest CH₃Hg production) was analyzed after using various purification protocols, alongside the standard CH₃Hg controls. Measured $\delta^{13}\text{C}$ values and the purification protocols applied are shown in Fig. S2 with more details in Table S2 of the SI. We observed that simple distillation alone was insufficient to eliminate C matrix interferences, as indicated by noisy chromatograms, while double distillation followed by gel preconcentration was found to be the most reliable method, yielding the best recoveries (Fig. S2).

For the biotically produced CH₃Hg, a consistent C isotope signature was observed across all samples, with an average $\delta^{13}\text{C}_{\text{CH}_3\text{Hg}}$ value of $-23.1 (\pm 2.0, \text{SD})$ ‰, independent of methylation yield as shown in Fig. 1. The constant $\delta^{13}\text{C}_{\text{CH}_3\text{Hg}}$, regardless of methylation yield, is the result of the large pyruvate C substrate pool, whose bulk $\delta^{13}\text{C}$ remains constant during the experiments. These values broadly align with the $\delta^{13}\text{C}$ range typical of biologically produced organic matter (-6 ‰ to -30 ‰³⁶). To provide further insight into the C isotope fractionation during iHg methylation, bulk C isotopic signatures ($\delta^{13}\text{C}_{\text{bulk}}$) of the BerOc1 pellets and organic components of the culture media were also measured and represented in Fig. 1 and detailed in Table 1.

Biotically produced CH₃Hg exhibited a ~9‰ ¹³C-depletion (lighter C isotope enrichment) relative to the bulk $\delta^{13}\text{C}$ of bacterial pellets and a ~14‰ depletion compared to the carbon source, pyruvate. No other components showed similar $\delta^{13}\text{C}$ values; CH₃Hg was ¹³C-enriched by ~8‰ and ~10‰ relative to the multivitamin V7 solution and fumarate,

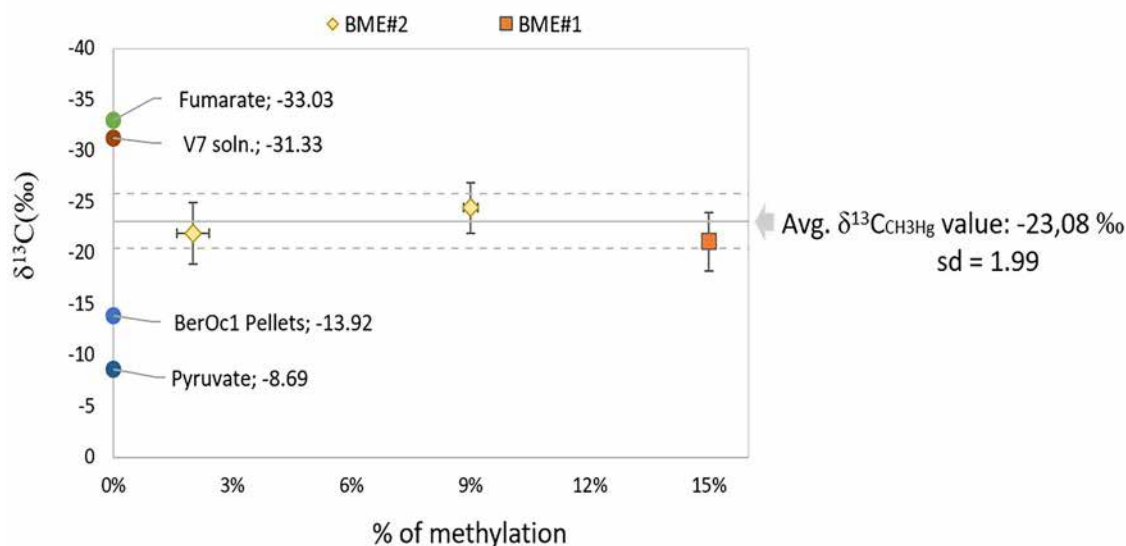
Biotic methylation: $\delta^{13}\text{C}$ vs % methylation

Fig. 1 | $\delta^{13}\text{C}$ (‰) values obtained for biotically produced CH_3Hg samples. The orange square represents the sample from BME#1 with 15% methylation, and the yellow diamonds represent the samples from the BME#2 with 2% and 9% of

methylation, respectively. Bulk $\delta^{13}\text{C}$ values from BerOc1 pellets, C source pyruvate, fumarate, and multivitamin solution (V7 soln.) containing vitamins B (1,3,5,6,8,10, and 12) are also shown.

Table 1 | Bulk C isotopic signatures ($\delta^{13}\text{C}_{\text{bulk}}$) from the pellets and the organic components of the culture media

| Sample name | Chemical formula/content | % of molecular weight as C | $\delta^{13}\text{C}_{\text{bulk}}$ (‰) |
|--|---|----------------------------|---|
| Sodium Pyruvate | $\text{C}_3\text{H}_3\text{NaO}_3$ | 33% | -8.69 |
| BerOc1 Pellets | whole cells from strain BerOc1 | ~50% | -13.92 |
| V7 Solution | Vitamins B (1, 3, 5, 6, 7, 10, 12) | ~55% | -31.33 |
| Sodium Fumarate | $\text{C}_4\text{H}_2\text{Na}_2\text{O}_4$ | 30% | -33.03 |
| Avg. $\delta^{13}\text{C}_{\text{CH}_3\text{Hg}} = -23.08 (\pm 1.99, \text{SD})$ ‰ | | | |

The average CSIA $\delta^{13}\text{C}_{\text{CH}_3\text{Hg}}$ from the biotic methylation samples is also shown.

respectively. In summary, the bacterial biomass was ~5‰ depleted in ^{13}C compared to pyruvate, while CH_3Hg showed a greater depletion of ~14‰ relative to pyruvate and ~9‰ relative to the biomass. These values provide preliminary, operational isotope fractionation factors for CH_3Hg production by *BerOc1*. A formal fractionation factor for methylation requires knowing the $\delta^{13}\text{C}$ of the unknown methyl donor group, which is position-specific and was not determined. We suggest that the ~9‰ depletion in $\delta^{13}\text{C}$ between C source and in vitro microbially produced CH_3Hg could be a potential analog for C isotope fractionation between natural organic carbon substrates and CH_3Hg in aquatic freshwater and marine ecosystems. Our observation of a ~9‰ depletion in $\delta^{13}\text{C}$ then opens the way to use biological tissue CH_3Hg $\delta^{13}\text{C}$ to understand the origin of the C source and methylation sites, such as terrestrial vs marine C, or water column vs sediment.

Discussion

The observed ^{13}C -depletion in biomass relative to substrates is consistent with previous studies^{37–39} and is typically attributed to enzymatic preference for lighter isotopes during key reactions such as decarboxylation and dehydrogenation⁴⁰. For example, up to 20‰ enrichment on the light C isotopes was observed for other organometals of biogenic origin in compost incubations³⁸. Additionally, not all carbon atoms from substrates contribute to biomass production^{41,42}, adding complexity to determining specific isotope fractionation during both biomass formation and iHg methylation.

While detailed mechanisms of iHg methylation in microbial cells remain unclear^{17,43}, early studies have explored connections between

metabolic pathways, corrinoids, and Hg methylation. Initial research using radiotracers suggested Hg methylation was part of carbon fixation pathways like the reductive acetyl-CoA (Wood–Ljungdahl, WL) pathway, with methyl-tetrahydrofolate ($\text{CH}_3\text{-H}_4\text{folate}$) as the methyl donor and cobalamin (vitamin B12) identified as the main corrinoid, along with a 40-kDa corrinoid protein^{10,14,33}. However, later findings indicated Hg methylation could occur independently of the acetyl-CoA pathway, particularly in microorganisms lacking this carbon fixation mechanism⁴⁴. The discovery of the *hgcAB* gene pair, essential for Hg methylation (with its deletion leading to a loss of methylation ability), shifted focus back to acetyl-CoA pathway-like models^{12,13,15}. The most used model representation of this Hg methylation mechanism is illustrated in Fig. 2.

Considering a reductive acetyl-CoA like pathway to describe the biotic methylation observed in *BerOc1*, several generalizations could help explain C isotope fractionation and its origin. For example, the methyl group (C1 precursor from Fig. 2) may originate from the carbon-3 amino acid serine, or its derivative folate as suggested in early studies¹⁰. This methyl group is then enzymatically transferred to tetrahydrofolate (THF) and subsequently to iHg via cobalamin-HgcAB protein complex^{12,14}. Serine biosynthesis typically derives from a phosphorylated form of pyruvate (Fig. 3)³³, which could link the C source in our experiments to the final methylated product, CH_3Hg . However, without detailed metabolic data for *BerOc1*, these connections remain speculative.

An important observation from this biotic methylation model (Fig. 2), assuming cobalamin as cofactor of the HgcA protein, is that it allows for

Fig. 2 | Most generalized pathway considered to explain enzymatic methylation of iHg. HgcA and HgcB are the proteins expressed from the gene cluster *hgcAB* considered to be essential for iHg methylation within the microbial cell. The $-\text{CH}_3$ group is obtained as part of the folate cycle, the most commonly used mechanism for single-carbon addition metabolism.

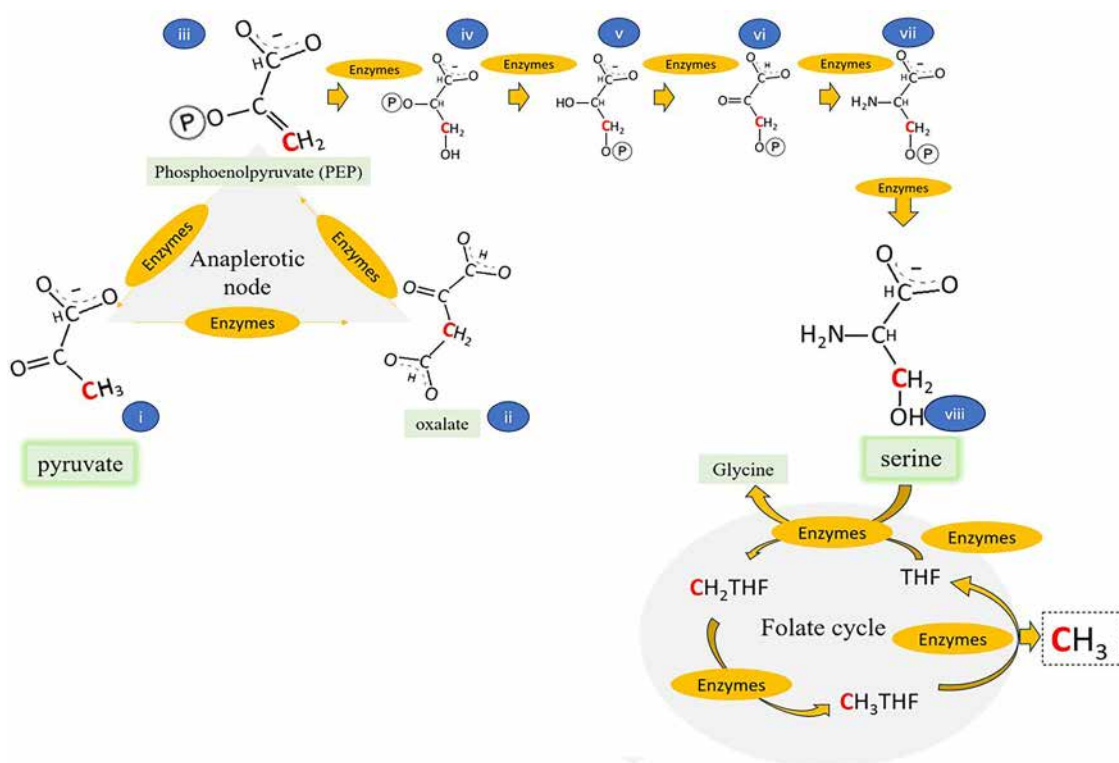
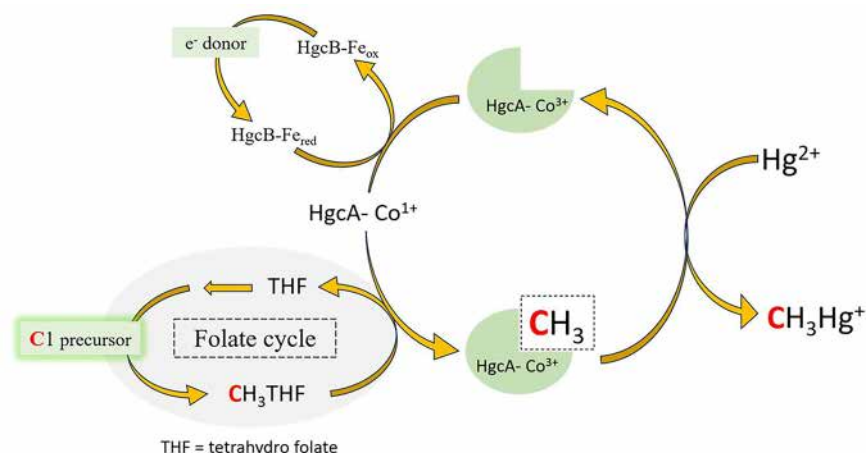


Fig. 3 | Biosynthesis of serine from pyruvate as proposed by Berman et al. In 1990³³. The C3 from pyruvate which is considered the one transferred as methyl group to iHg is represented in bold and red. Compounds represented are: i-) pyruvate, ii-) oxalate, iii-) phosphoenolpyruvate, iv-) 2-phosphoglycerate; v-) 3-phosphoglycerate; vi-) 3-phosphohydroxypyruvate; vii-) phosphoserine; viii-) serine.

Afterwards, the serine enters in the serine/glycine synthesis and the folate cycle as the main single C addition mechanism in many living beings. C3 from serine is added to tetrahydrofolate (THF) to form $\text{CH}_3\text{-THF}$ and then used for single C addition metabolisms.

repeated methylation and demethylation of the same cobalamin molecule, enabling high methylation yields even with low vitamin B12 concentrations—unlike what has been observed in abiotic methylation experiments with methylcobalamin^{45,46}. The C isotope fractionation related to this process is, however, difficult to establish without further specific metabolic information on BerOcl strain. In addition, biotic demethylation can potentially alter the C isotopic signature of CH_3Hg in aquatic environments, as shown for Hg isotopes. Demethylation (biotic and photo-demethylation) has been observed to enrich both heavier Hg and C isotopes in the remaining CH_3Hg fraction, as lighter isotopes are preferentially removed^{26,32}. Future work should therefore investigate carbon isotope fractionation during biotic CH_3Hg demethylation.

Pyruvate, a key metabolic node, is regulated by numerous intrinsic and extrinsic factors⁴⁷. Assuming the $-\text{CH}_3$ group originates from pyruvate as proposed by Berman et al. in 1990³³, through the pyruvate→oxaloacetate→PEP→serine→5- $\text{CH}_3\text{-THF}$ pathway (Fig. 3), the interconnected metabolic reactions must be considered, especially since the PEP–pyruvate–oxaloacetate node (also known as anaplerotic node) is a switch point in major metabolic pathways⁴⁸. This node integrates diverse essential reactions, with enzymes adjusting carbon fluxes based on cellular demands, and shifting functions under different conditions^{49,50}. The enzymes at this anaplerotic node form a complex regulatory network ensuring optimal C and energy flow⁵¹.

As mentioned above, it is considered that iHg methylation is the result of a one-C addition mechanism inside bacteria¹³, but the precise link between C isotope fractionation from the C source to CH₃Hg is challenging to identify. The serine/glycine biosynthesis pathway and the folate cycle (Fig. 3) are typically involved in the one-carbon addition metabolism, generating carbon units for various metabolic demands, including nucleotide biosynthesis and methylation reactions⁵². Serine can be either taken up by the cell or biosynthesized from pyruvate derivatives. As early as 1990, it was proposed that this pathway was responsible for mercury methylation in *Desulfovibrio desulfuricans*³³. However, the specific methylation pathway may vary between strains, as both autotrophic and heterotrophic mechanisms for synthesizing cellular material have been identified in sulfate-reducing bacteria (SRB), including species of *Desulfovibrio*^{41,44,53}. This suggests that the pathway of the transfer of the methyl (-CH₃) group could differ based on strain-specific metabolic capabilities.

The *hgcAB* gene cluster encodes a methylating system that facilitates Hg methylation in all known methylating microorganisms, but the exact mechanism remains unclear¹⁶. Although these genes enable Hg efflux, they are not induced by Hg exposure, and their deletion in strains like *Pseudodesulfovibrio mercurii* ND132 and *Geobacter sulfurreducens* PCA does not affect growth or central metabolism^{13,54}. This suggests that Hg methylation may be a specialized or incidental process, with Hg possibly entering an unknown methylation substrate. The presence of the *hgcAB* gene pair in microbial genomes might be environmentally regulated¹⁶, further complicating the estimation of metabolically induced carbon isotope fractionation.

Isotope fractionation from enzymatically catalyzed biosynthetic processes is primarily driven by enzyme-mediated reactions rather than the isotope mass itself^{39,40,55}. Enzymes often discriminate against heavier isotopes like ¹³C, leading to isotope fractionation but they also induce position-specific isotope effects, where particular bonds in molecules (often in intermediates) are more prone to isotope fractionation depending on the reaction mechanisms³⁹. The observed $\delta^{13}\text{C}$ fractionation from pyruvate to CH₃Hg by BerOc1 in the present study could then be the result of preferential usage of specific carbon positions in pyruvate during fermentation or other metabolic reactions under anoxic conditions, as suggested in previous studies^{33,38,42}.

Studies on carbon isotope fractionation in heterotrophs, particularly related to highly specific mechanisms like Hg methylation, are limited. In our research, no direct $\delta^{13}\text{C}$ measurements of the methyl group in biotically produced CH₃Hg have been reported to our knowledge. However, our observations align with previous work on fractionation in the acetyl-CoA pathway and sulfate-reducing bacteria (SRB). Studies of carbon fixation across different bacterial mechanisms show diverse and substantial fractionation, often depending on the carbon fixation route and the targeted substrate. A common finding is significant isotope fractionation in the biomass of organisms using the acetyl-CoA pathway relative to the carbon source^{39,41,56}. However, observed fractionation varies widely, from ~3‰ to over 35‰, making it difficult to use as a definitive marker, highlighting the need for further study to identify metabolic pathways involved in methylation.

Summarizing, we observed a ¹³C-depletion of ~5‰ in the biomass of *Pseudodesulfovibrio hydrargyri* strain BerOc1 compared to the C source (pyruvate) used, a ~14‰ depletion in CH₃Hg relative to pyruvate, and a ~9‰ depletion relative to biomass. We suggest that the ~9‰ depletion in $\delta^{13}\text{C}$ between C source and in vitro microbially produced CH₃Hg could be a potential analog for C isotope fractionation between natural dissolved organic carbon substrates and CH₃Hg in aquatic freshwater and marine ecosystems. These values are consistent with isotope fractionation factors reported in other carbon flux studies, but currently it is not possible to establish a specific carbon fixation pathway or the precise origin of C in iHg methylation, due to the complex enzymatic reactions involved. We consider that the methyl group for Hg methylation in BerOc1 may originate from pyruvate via a metabolic network involving the serine pathway and folate cycle, as previously suggested for *Desulfovibrio desulfuricans*. However, elucidating the pathways is challenging due to the intricate nature of

enzyme-mediated carbon isotope fractionation, which is influenced more by enzyme specificity and catalytic efficiency than simple isotope effects. Further elucidation on BerOc1 metabolism and more studies using different methylators is still required.

Methods

For this study, CH₃Hg produced from two separate biotic methylation experiments (BME) was utilized. Both experiments were conducted at the IPREM (Institute of Analytical Sciences and Physico-Chemistry for Environment and Materials, Pau, France), using the same strain and reagents, under non-sulfidogenic growth conditions (pyruvate/fumarate). BME#1 was performed as part of a previous study with an initial OD of 0.04, while BME#2 was conducted as part of a larger experiment for the present research with an initial OD of 0.02. The specific experimental conditions are summarized below.

BerOC1 strain and culture growth conditions

The SRB *Pseudodesulfovibrio hydrargyri* strain BerOc1, isolated in 2004 from sediments of a brackish lagoon (Etang de Berre, southeast France)⁵⁷, was used in this study. The strain was routinely pre-cultivated during the week before the experiment in an anoxic liquid medium at approximately 37°C, with a pH of ~7, and dark conditions. Purity and growth of the strain were confirmed by multiple phase contrast microscope observations (BX60, Olympus) and through measurements of optical density (OD) at 600 nm.

For experimental incubations, a multipurpose medium (MM10⁵⁸) was prepared, containing per liter: 10 g NaCl, 1.2 g MgCl₂·6H₂O, 0.1 g CaCl₂·2H₂O, 0.25 g NH₄Cl, 0.5 g KCl, and 2.6 g of HEPES. Additionally, 1 mL each of a trace elements solution (SL12B⁵⁹), a selenite-tungstate solution, and a multivitamin solution (V7⁶⁰) were added. Cultures were grown using pyruvate as the C source alongside fumarate respiration to ensure a non-sulfidogenic metabolism. The pyruvate-fumarate combination was selected to promote a bacterial metabolism capable of sufficient iHg methylation yields for C isotope analysis²³. These substrates were prepared in degassed MQ water and added to incubation vials to obtain final concentrations of 40 mM each, marking the start of the incubation period.

Cultures were inoculated at an initial OD of 0.04 and 0.02 for BME#1 and BME#2, respectively, from pre-cultures to grow under identical conditions. Growth was monitored by measuring OD at 600 nm, and biomass production (ΔOD_{600}) was calculated using Eq. 1:

$$\Delta\text{OD}_{600} = [\text{OD}_{\text{tf}} - \text{OD}_{\text{ti}}] \quad (1)$$

Where OD_{tf} is the optical density at the end of the exponential phase and OD_{ti} is the optical density at the beginning of the inoculation. The growth rate, $\mu = (\ln\text{OD}_{\text{tf}} - \ln\text{OD}_{\text{ti}})/(\text{tf} - \text{ti})$ (h⁻¹) was then determined by dividing the natural logarithm of biomass production during the exponential phase by the duration of the exponential growth phase.

iHg addition and incubation time

Samples were incubated individually in 50 mL crimp-sealed glass vials. For cultures exposed to iHg, mercury (II) chloride (HgCl₂) at natural isotopic abundance in 1% hydrochloric acid (HCl) was added to the vials before inoculating with the BerOc1 strain, following similar procedures as previous studies^{23,26}. Control samples, without the addition of Hg, were incubated for 30 h under identical conditions to serve as matrix blanks for subsequent analyses. An additional control sample with inactive cells was incubated for 30 h to assess any potential abiotic iHg methylation. All samples were incubated in triplicate for predetermined durations. To stop the methylation process, the medium was acidified with bi-distilled nitric acid (~15 N). From BME#1, two samples were collected at 24 h, one corresponding to the condition of addition of iHg and the other to absence of iHg. From BME#2, triplicate samples were collected at 0 h, 4 h, 8 h, and 30 h for isotopic analysis. Further details on the samples and conditions are provided in Table 2.

Table 2 | Composition of the samples analyzed during our study. Initial OD of 0.04 and 0.02 for BME#1 and BME#2 respectively

| Experiments | Incubation time | Conditions | | |
|---------------|-----------------|-------------------------------------|-------------------|------------------------|
| | | active cells + no Hg | active cells + Hg | inactive cells + Hg |
| BME 1 | ~24 h | 1 sample | 1 sample | — |
| BME 2 | 0 h | 3 samples ^a | 3 samples | — |
| | 4 h | — | 3 samples | — |
| | 8 h | — | 3 samples | — |
| | 30 h | 3 samples | 3 samples | 3 samples ^a |
| 2 Experiments | | 17 samples in total for carbon CSIA | | |

^anot analyzed for C isotopes.

Sample processing and analysis

The acidified samples were digested on a hot plate at 90 °C for 4 h before analysis. For total mercury (THg) concentration analysis, a portion of the digested sample was diluted with 10% (v/v) aqueous HCl and bromine monochloride (BrCl). THg concentrations were then measured using cold-vapor atomic fluorescence spectrometry (CV-AFS). For mercury speciation, an aliquot of the digested sample was diluted in 40 mL of buffered Milli-Q water (pH ~5) and analyzed using Purge and Trap-Gas Chromatography-Cold Vapor Atomic Fluorescence Spectrometry (PT-GC-CVAFS) after derivatization with sodium tetra-ethyl borate (NaBEt₄). Additionally, the methodology described by Kleindienst et al. 2023⁶¹ was used in non-acidified samples to determine methylated Hg species in the samples.

CH₃Hg compound specific isotope analysis (CSIA) of C stable isotopes was performed in this study at the Géosciences Environnement Toulouse laboratory (France). For C CSIA, BerOc1 culture aliquot samples were neutralized with concentrated (~15 N) NaOH and distilled once or twice to separate CH₃Hg from potential interferents, following the procedure described by Rosera et al.⁶². THg concentration and Hg speciation were analyzed before and after each distillation and pre-concentration step. After the successive neutralizations and distillations, the samples with CH₃Hg concentrations below 7 ng/g were pre-concentrated using binding gels composed of polyacrylamide crosslink agarose with 3MFS (3-mercaptopropyl functionalized silica) resin (supplied by DGT® Research).

To assess any matrix effects and potential carbon isotope fractionation induced by these purification and separation processes, we analyzed our in-house CH₃Hg chloride standard^{30,31} in Milli-Q water and in biotic methylation blanks (containing cells and culture media without iHg addition). Triplicate CH₃Hg controls in Milli-Q water and matrix blanks were processed in parallel with each sample, following the exact preparation procedures applied to the samples. Finally, CSIA of C isotopes was performed using Purge and Trap-Gas Chromatography-Combustion-Isotope Ratio Mass Spectrometry (PT-GC-C-IRMS) for all samples with sufficient CH₃Hg concentration, along with corresponding CH₃Hg standard controls.

For bulk δ¹³C analysis of BerOc1 pellets and the organic compounds used (fumarate, pyruvate, V7) in the culture media, a continuous flow mass spectrometer (Delta V, Thermo Scientific, Germany) coupled to an elemental analyzer (Flash EA 2000, Thermo Scientific, Italy) was used at the Pôle Spectrométrie Océan (IUEM, CNRS, IRD, Plouzané, France). To prepare for this analysis, 3–5 g of the fumarate and pyruvate substrates were transferred into 5 mL Eppendorf tubes, and approximately 5 mL of the stock multi-vitamin solution (V7) was freeze-dried for two days. Pellets (BerOc1 cells) were grown in 2 L of MM10 medium, centrifuged to separate the cells from the supernatant, rinsed, frozen at -80 °C to preserve cell integrity, and freeze-dried for two days before being sent for bulk carbon isotope analysis.

Calculations

The rate constant (k_m) for the iHg methylation reaction was estimated using a simplified irreversible pseudo-first-order model. Although the

BerOc1 strain is known to demethylate CH₃Hg, we considered only the irreversible methylation process due to our inability to quantify demethylation during the experiments, since unlike other studies²⁶, only Hg with natural abundance isotopic composition was used. Moreover, during our experiments, methylation appeared to dominate, as CH₃Hg concentrations consistently increased over time (Fig. S1A). We then considered that the duration of the experiment was short enough to use the simplification of $k(\text{methylation of Hg}^{2+}) \gg k(\text{demethylation of CH}_3\text{Hg})$ ¹⁶.

The k_m was determined by calculating the slope from the best linear fit of the natural logarithm (\ln) of the remaining fraction of iHg species ($f[iHg]_r$) over time, as shown in Eq. 2:

$$\ln(f[iHg]_r) = -k_m \times t \quad (2)$$

The remaining fraction of iHg over time was calculated based on the observed increase in CH₃Hg concentration, rather than the decrease in iHg, due to the challenges in accurately measuring the reduction in reactant concentration. The approximation used to estimate $f[iHg]_r$ is shown in Eq. 3:

$$f(iHg)_{\text{remaining}} = \frac{[iHg]_t}{[iHg]_{t_0}} \approx 1 - f(iHg)_{\text{methylated}} \approx 1 - f(\text{CH}_3\text{Hg})_{\text{formed}} \quad (3)$$

The fraction of CH₃Hg formed was calculated as the ratio of the observed CH₃Hg concentration at time t to the THg concentration measured in the sample. The measured THg concentration was used, rather than the expected concentration based on the initial iHg added, due to varying degrees of iHg loss, which affected differently the THg levels in each incubation vial. Similar iHg loss has been observed before in biotic methylation cultures, mainly attributed to factors like HgS(s) formation, vessel wall adsorption, or Hg⁰ formation^{23,63,64} but was considered not important for our study since Hg isotope fractionation wasn't directly analyzed. For the same reasons, the methylation yields for C isotope analysis were also calculated based on the THg concentrations measured in each sample rather than the THg expected concentration. This also was carried on to ensure same considerations between the two different experiments analyzed in this work. For more information on the percentages of methylation and THg recovery, see table S1 on the S1.

Data availability

All relevant data supporting the findings of this study are included in the main manuscript and the Supplementary Information.

Received: 27 May 2025; Accepted: 12 July 2025;

Published online: 29 July 2025

References

- Compeau, G. C. & Bartha, R. Sulfate-reducing bacteria: principal methylators of mercury in anoxic estuarine sediment. *Appl. Environ. Microbiol.* **50**, 498–502 (1985).
- Vigneron, A., Cruaud, P., Aubé, J., Guyoneaud, R. & Goñi-Urriza, M. Transcriptomic evidence for versatile metabolic activities of mercury cycling microorganisms in brackish microbial mats. *NPJ Biofilms Microbiomes* **7**, 83 (2021).
- Peng, X., Yang, Y., Yang, S., Li, L. & Song, L. Recent advance of microbial mercury methylation in the environment. *Appl. Microbiol. Biotechnol.* **108**, 235 (2024).
- Barton, L. L. & Fauque, G. D. Biochemistry, physiology and biotechnology of sulfate-reducing bacteria. In *Advances in Applied Microbiology* Vol. 68, Ch. 2, (2009).
- Muyzer, G. & Stams, A. J. M. The ecology and biotechnology of sulphate-reducing bacteria. *Nat. Rev. Microbiol.* **6**, 441–454 (2008).
- Plugge, C. M., Zhang, W., Scholten, J. C. M. & Stams, A. J. M. Metabolic flexibility of sulfate-reducing bacteria. *Front. Microbiol.* **2** (2011).

7. Liamleam, W. & Annachhatre, A. P. Electron donors for biological sulfate reduction. *Biotechnol. Adv.* **25**, 452–463 (2007).
8. Qian, Z., Tianwei, H., Mackey, H. R., van Loosdrecht, M. C. M. & Guanghao, C. Recent advances in dissimilatory sulfate reduction: from metabolic study to application. *Water Res.* **150**, 162–181 (2019).
9. Wood, J. M., Kennedy, F. S. & Rosen, C. G. Synthesis of methylmercury compounds by extracts of a methanogenic bacterium. *Nature* **220**, 173–174 (1968).
10. Choi, S. C., Chase, T. & Bartha, R. Enzymatic catalysis of mercury methylation by *Desulfovibrio desulfuricans* LS. *Appl. Environ. Microbiol.* **60**, 1342–1346 (1994).
11. Isaure, M. P. et al. Relationship between Hg speciation and Hg methylation/demethylation processes in the sulfate-reducing bacterium *Pseudodesulfovibrio hydrargyri*: evidences from HERFD-XANES and Nano-XRF. *Front. Microbiol.* **11**, 584715 (2020).
12. Cooper, C. J. et al. Structure determination of the HgcAB complex using metagenome sequence data: insights into microbial mercury methylation. *Commun. Biol.* **3**, 320 (2020).
13. Parks, J. M. et al. The genetic basis for bacterial mercury methylation. *Science* **339**, 1332–1335 (2013).
14. Choi, S. C. & Bartha, R. Cobalamin-mediated mercury methylation by *Desulfovibrio desulfuricans* LS. *Appl. Environ. Microbiol.* **59**, 290–295 (1993).
15. Date, S. S. et al. Kinetics of enzymatic mercury methylation at nanomolar concentrations catalyzed by HgcAB. *Appl. Environ. Microbiol.* **85**, e00438-19 (2019).
16. Regnell, O. & Watras, C. J. Microbial mercury methylation in aquatic environments: a critical review of published field and laboratory studies. *Environ. Sci. Technol.* **53**, 4–19 (2019).
17. Bravo, A. G. & Cosio, C. Biotic formation of methylmercury: a bio-physico-chemical conundrum. *Limnol. Oceanogr.* **65**, 1010–1027 (2020).
18. Ranchou-Peyruse, M. et al. Overview of mercury methylation capacities among anaerobic bacteria including representatives of the sulphate-reducers: implications for environmental studies. *Geomicrobiol. J.* **26**, 1–8 (2009).
19. Bridou, R., Monperrus, M., Rodriguez-Gonzalez, P., Guyoneaud, R. & Amouroux, D. Simultaneous determination of mercury methylation and demethylation capacities of various sulfate-reducing bacteria using species-specific isotopic tracers. *Environ. Chem.* **30**, 337–344 (2011).
20. Gilmour, C. C. et al. Sulfate-reducing bacterium *Desulfovibrio desulfuricans* ND132 as a model for understanding bacterial mercury methylation. *Appl. Environ. Microbiol.* **77**, 3938–3951 (2011).
21. Goñi-Urriza, M. et al. Relationships between bacterial energetic metabolism, mercury methylation potential, and hgcA/hgcB gene expression in *Desulfovibrio dechloroacetivorans* BerOc1. *Environ. Sci. Pollut. Res.* **22**, 13764–13771 (2015).
22. Ranchou-Peyruse, M. et al. *Pseudodesulfovibrio hydrargyri* sp. nov., a mercury-methylating bacterium isolated from a brackish sediment. *Int. J. Syst. Evol. Microbiol.* **68**, 1461–1466 (2018).
23. Barrouilhet, S. et al. Effect of exogenous and endogenous sulfide on the production and the export of methylmercury by sulfate-reducing bacteria. *Environ. Sci. Pollut. Res.* **30**, 3835–3846 (2023).
24. Goñi-Urriza, M., Gassie, C., Bouchez, O., Klopp, C. & Guyoneaud, R. Draft genome sequence of *Desulfovibrio* BerOc1, a mercury-methylating strain. *Genome Announc.* **5**, (2017).
25. Pedrero, Z. et al. Transformation, localization, and biomolecular binding of Hg species at subcellular level in methylating and nonmethylating sulfate-reducing bacteria. *Environ. Sci. Technol.* **46**, 11744–11751 (2012).
26. Perrot, V. et al. Identical Hg isotope mass dependent fractionation signature during methylation by sulfate-reducing bacteria in sulfate and sulfate-free environment. *Environ. Sci. Technol.* **49**, 1365–1373 (2015).
27. Bergquist, B. A. & Blum, J. D. Mass-dependent and -independent fractionation of Hg isotopes by photoreduction in aquatic systems. *Sci. Rep.* **318**, 417–420 (2007).
28. Tsui, M. T.-K., Blum, J. D. & Kwon, S. Y. Review of stable mercury isotopes in ecology and biogeochemistry. *Sci. Total Environ.* **716**, 135386 (2020).
29. Janssen, S. E., Schaefer, J. K., Barkay, T. & Reinfelder, J. R. Fractionation of mercury stable isotopes during microbial methylmercury production by iron- and sulfate-reducing bacteria. *Environ. Sci. Technol.* **50**, 8077–8083 (2016).
30. Masbou, J. et al. Carbon stable isotope analysis of methylmercury toxin in biological materials by gas chromatography isotope ratio mass spectrometry. *Anal. Chem.* **87**, 11732–11738 (2015).
31. Queipo-Abad, S., Lagane, C. & Point, D. Sensitive determination of methylmercury $\delta^{13}\text{C}$ compound specific stable isotopic analysis by purge and trap gas chromatography combustion isotope ratio mass spectrometry. *J. Chromatogr. A* **1617**, 460821 (2020).
32. Malberti-Quintero, L. M., Sonke, J. E., Lagane, C., Laffont, L. & Point, D. Carbon and mercury stable isotope fractionation during aqueous photodemethylation of CH_3Hg . *ACS EST Water* **5**, 556–565 (2025).
33. Berman, M., Chase, T. & Bartha, R. Carbon flow in mercury biomethylation by *Desulfovibrio desulfuricans*. *Appl. Environ. Microbiol.* **56**, 298–300 (1990).
34. Schaefer, J. K. et al. Active transport, substrate specificity, and methylation of Hg(II) in anaerobic bacteria. *Proc. Natl. Acad. Sci. USA* **108**, 8714–8719 (2011).
35. Rodríguez Martín-Doimeadios, R. C. et al. Mercury methylation/demethylation and volatilization pathways in estuarine sediment slurries using species-specific enriched stable isotopes. *Mar. Chem.* **90**, 107–123 (2004).
36. Berto, D. et al. Elemental analyzer/isotope ratio mass spectrometry (EA/IRMS) as a tool to characterize plastic polymers in a marine environment. In *Plastics in the Environment* (IntechOpen, <https://doi.org/10.5772/intechopen.81485> (2019).
37. Zhuang, G.-C. et al. Distribution and isotopic composition of trimethylamine, dimethylsulfide and dimethylsulfoniopropionate in marine sediments. *Mar. Chem.* **196**, 35–46 (2017).
38. Wuerfel, O., Diaz-Bone, R. A., Stephan, M. & Jochmann, M. A. Determination of $^{13}\text{C}/^{12}\text{C}$ isotopic ratios of biogenic organometal(loid) compounds in complex matrixes. *Anal. Chem.* **81**, 4312–4319 (2009).
39. Hayes, J. M. 3. Fractionation of carbon and hydrogen isotopes in biosynthetic processes. In *Stable Isotope Geochemistry* 225–278 (De Gruyter, <https://doi.org/10.1515/9781501508745-006> (2001).
40. Fry, B. *Stable Isotope Ecology*. vol. 521 (Springer, 2006).
41. Govert, D. & Conrad, R. Carbon Isotope Fractionation by Sulfate-Reducing Bacteria Using Different Pathways for the Oxidation of Acetate. *Environ. Sci. Technol.* **42**, 7813–7817 (2008).
42. Dijkstra, P. et al. Probing carbon flux patterns through soil microbial metabolic networks using parallel position-specific tracer labeling. *Soil Biol. Biochem.* **43**, 126–132 (2011).
43. Hsu-Kim, H., Kucharzyk, K. H., Zhang, T. & Deshusses, M. A. Mechanisms regulating mercury bioavailability for methylating microorganisms in the aquatic environment: a critical review. *Environ. Sci. Technol.* **47**, 2441–2456 (2013).
44. Ekstrom, E. B., Morel, F. M. M. & Benoit, J. M. Mercury methylation independent of the acetyl-coenzyme A pathway in sulfate-reducing bacteria. *Appl. Environ. Microbiol.* **69**, 5414–5422 (2003).
45. Jiménez-Moreno, M., Perrot, V., Epov, V. N., Monperrus, M. & Amouroux, D. Chemical kinetic isotope fractionation of mercury during abiotic methylation of Hg(II) by methylcobalamin in aqueous chloride media. *Chem. Geol.* **336**, 26–36 (2013).
46. Filippelli, M. & Baldi, F. Alkylation of ionic mercury to methylmercury and dimethylmercury by methylcobalamin: simultaneous determination by purge-and-trap GC in line with FTIR. *Appl. Organomet. Chem.* **7**, 487–493 (1993).

47. Prochownik, E. V. & Wang, H. The metabolic fates of pyruvate in normal and neoplastic cells. *Cells* **10**, 762 (2021).
48. Yin, L., Zhou, Y., Ding, N. & Fang, Y. Recent advances in metabolic engineering for the biosynthesis of phosphoenol pyruvate–oxaloacetate–pyruvate-derived amino acids. *Molecules* **29**, 2893 (2024).
49. Koendjibiharie, J. G., van Kranenburg, R. & Kengen, S. W. M. The PEP–pyruvate–oxaloacetate node: variation at the heart of metabolism. *FEMS Microbiol. Rev.* **45**, (2021).
50. Stryer, L. *Biochemistry*. 3rd edn (W. H. Freeman & Company, 1975).
51. Sauer, U. & Eikmanns, B. J. The PEP—pyruvate—oxaloacetate node as the switch point for carbon flux distribution in bacteria: We dedicate this paper to Rudolf K. Thauer, Director of the Max-Planck-Institute for Terrestrial Microbiology in Marburg, Germany, on the occasion of his 65th birthday. *FEMS Microbiol. Rev.* **29**, 765–794 (2005).
52. Pan, S., Fan, M., Liu, Z., Li, X. & Wang, H. Serine, glycine and one-carbon metabolism in cancer (Review). *Int. J. Oncol.* **58**, 158–170 (2020).
53. Schauder, R., Preu, A., Jetten, M. & Fuchs, G. Oxidative and reductive acetyl CoA/carbon monoxide dehydrogenase pathway in *Desulfobacterium autotrophicum*. *Arch. Microbiol.* **151**, 84–89 (1988).
54. Yu, R.-Q., Reinfelder, J. R., Hines, M. E. & Barkay, T. Mercury methylation by the methanogen *Methanospirillum hungatei*. *Appl. Environ. Microbiol.* **79**, 6325–6330 (2013).
55. Sharp, Zachary. *Principles of Stable Isotope Geochemistry*. (2017).
56. House, C. H., Schopf, J. W. & Stetter, K. O. Carbon isotopic fractionation by Archaeans and other thermophilic prokaryotes. *Org. Geochem.* **34**, 345–356 (2003).
57. Ranchou-Peyruse, A. et al. Characterization of brackish anaerobic bacteria involved in hydrocarbon degradation: a combination of molecular and culture-based approaches. *Ophelia* **58**, 255–262 (2004).
58. Widdel, F. & Bak, F. Gram-Negative mesophilic sulfate-reducing bacteria. In *The Prokaryotes* 3352–3378, https://doi.org/10.1007/978-1-4757-2191-1_21 (Springer New York, 1992).
59. Overmann, J., Fischer, U. & Pfennig, N. A new purple sulfur bacterium from saline littoral sediments, *Thiorhodovibrio winogradskyi* gen. nov. and sp. nov. *Arch. Microbiol.* **157**, 329–335 (1992).
60. Trüper, H. G. & Pfennig, N. The family Chlorobiaceae. In *The Prokaryotes* 3583–3592, https://doi.org/10.1007/978-1-4757-2191-1_33 (Springer New York, 1992).
61. Kleindienst, A. et al. Assessing comparability and uncertainty of analytical methods for methylated mercury species in seawater. *Anal. Chim. Acta* **1278**, 341735 (2023).
62. Rosera, T. J. et al. Isolation of methylmercury using distillation and anion-exchange chromatography for isotopic analyses in natural matrices. *Anal. Bioanal. Chem.* **412**, 681–690 (2020).
63. Rodríguez-González, P. et al. Species-specific stable isotope fractionation of mercury during Hg(II) methylation by an anaerobic bacteria (*Desulfobulbus propionicus*) under dark conditions. *Environ. Sci. Technol.* **43**, 9183–9188 (2009).
64. Song, Y. et al. Toward an internally consistent model for hg(ii) chemical speciation calculations in bacterium–natural organic matter–low molecular mass thiol systems. *Environ. Sci. Technol.* **54**, 8094–8103 (2020).

Acknowledgements

This project has received funding from the European Union’s Horizon 2020 research and innovation program under the Marie Skłodowska-Curie grant agreement No 197100. J. X. acknowledges the doctoral fellowship funded by I-SITE E2S UPPA.

Author contributions

All authors reviewed and contributed to the preparation of the manuscript. LMM-Q drafted the main text of the manuscript and prepared the figures and tables.

Competing interests

The authors declare no competing interests.

Additional information

Supplementary information The online version contains supplementary material available at <https://doi.org/10.1038/s41545-025-00500-3>.

Correspondence and requests for materials should be addressed to Luisa M. Malberti-Quintero or David Point.

Reprints and permissions information is available at <http://www.nature.com/reprints>

Publisher’s note Springer Nature remains neutral with regard to jurisdictional claims in published maps and institutional affiliations.

Open Access This article is licensed under a Creative Commons Attribution-NonCommercial-NoDerivatives 4.0 International License, which permits any non-commercial use, sharing, distribution and reproduction in any medium or format, as long as you give appropriate credit to the original author(s) and the source, provide a link to the Creative Commons licence, and indicate if you modified the licensed material. You do not have permission under this licence to share adapted material derived from this article or parts of it. The images or other third party material in this article are included in the article’s Creative Commons licence, unless indicated otherwise in a credit line to the material. If material is not included in the article’s Creative Commons licence and your intended use is not permitted by statutory regulation or exceeds the permitted use, you will need to obtain permission directly from the copyright holder. To view a copy of this licence, visit <http://creativecommons.org/licenses/by-nc-nd/4.0/>.

© The Author(s) 2025